

# Investigating the Geomorphic Evidence and Movement Potential of Active Faults in Golpayegan Area, Iran

Nafiseh Hajnorouzi<sup>a,\*</sup>, Mohsen Pourkermani<sup>b,\*\*</sup>, Mehran Arian<sup>a</sup>, Zahra Maleki<sup>a</sup>, and Ali Solgi<sup>a</sup>

Received December 19, 2023; revised March 18, 2024; accepted March 25, 2024

**Abstract**—Along the western part of Golpayegan city, in an area parallel to the main axis of Zagros, the calculation of morphometric indices in the Golpayegan basin means that the tectonic activity is significant from a morphometric point of view. Tectonic activity was not the same throughout the region and although no major earthquake was reported in Golpayegan region, morphometric evidence shows the general tectonic activity of the region. Geomorphic evaluation of the Golpayegan area shows that some of the northwest-southeast trending faults and the tips of some faults in the west Golpayegan city should be considered as potential earthquake areas. The Golpayegan area is located in the Sanandaj-Sirjan structural zone, one of Iran's most active seismic zones. The present study aimed to evaluate the effect of faults on landforms through morphotectonic indices and the causes of knick points and knick zones in the Bedrock Rivers in part of the Sanandaj-Sirjan tectonic zone. To this end, six morphometric indices such as longitudinal gradient ( $SL$ ), hierarchical anomaly ( $\Delta a$ ), the bifurcation index ( $R$ ), hypsometric integral and hypsometric curve (Hi-Hc), relative relief ( $Bh$ ), and basin shape ( $Bs$ ) were calculated and analyzed in 22 sub-basins of the area. Based on the findings, the existence of slope-break knick points at the mountain piedmont and at the outlet of large rivers through active faults demonstrated these landforms were created by movements along the main faults such as Bid Arab and Khansar faults which have the highest mobility potential.

**Keywords:** active fault, movement potential, Khansar fault, morphotectonic, Golpayegan, Iran

**DOI:** 10.1134/S1028334X23603590

## INTRODUCTION

The Golpayegan drainage basin is located in Sanandaj-Sirjan metamorphic zone (SSMZ) of Iran and in the northeastern margin of the Zagros Mountains Ranges and southwest of Central Iranian volcanic belt. SSMZ, a metamorphic belt (150–250 km width and about 1500 km length) that is mainly composed of highly deformed rocks, extending for around 1500 km in NW–SE direction, was related to the destruction of the subducted Tethys Ocean followed by the collision of Arabian and Eurasian continental plates. SSMZ in Golpayegan region is divided into two parts [1]. The northern part, deformed in the Jurassic–Early Cretaceous and the Southern part consists of both Paleozoic units and a Carboniferous–Permian mafic and ultramafic complex. Polyphase deformation structures of SSMZ are attributed to dextral

transpression that is related to the oblique convergence between the Arabian – Eurasian continental plates [2]. On the other hand, subduction of the Oman oceanic crust besides Arabian collision, confined Cimmerian plate to have numerous active faults spread out over the large zones e.g. Zagros, Central Iranian plateau and Makran accretionary wedges. The non-occurrence of devastating earthquakes in this area could cause Golpayegan to be assumed as one of the passive areas of SSMZ, while the existence of some faults with NW–SE and NE–SW trends, parallel or perpendicular to the main Zagros thrust fault trend, made a question mark on this.

The trend of the mountain ranges of the study area is approximately northwest-southeast. The highest point above sea level is the Panj-Panje peak located in the south of Khansar, with a height of 3710 meters, and the city of Golpayegan, with a height of 1780 meters, is the lowest area in the range.

The Iranian plateau is an accumulation of various continental fragments that separated from the passive Gondwana margin, moved thousands of kilometers, and joined the Eurasian margin during various collisional events since the Late Neoproterozoic. The last complex tectonic events are simultaneous with the convergence of the Arabian and Eurasian plates. The

<sup>a</sup> Department of Earth Sciences, Faculty of Converging Sciences and Technologies, Science and Research Branch, Islamic Azad University, Tehran, Iran

<sup>b</sup> Department of Geology, North Tehran Branch, Islamic Azad University, Tehran, Iran

\*e-mail: n.hajnorouzi@srbiau.ac.ir

\*\*e-mail: m\_pourkermani@iau-tnb.ac.ir

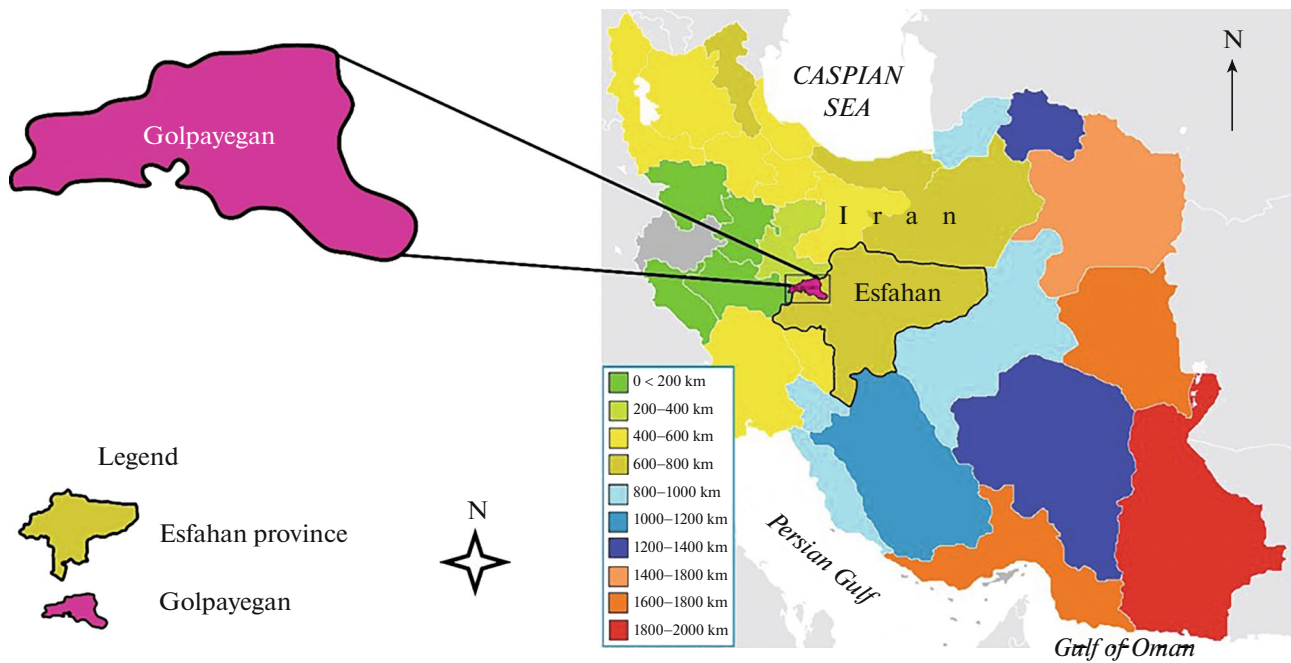


Fig. 1. Location of the study area in Iran.

aforementioned deformation is concentrated along the boundaries of microplates and in some areas covered by Cenozoic magmatic arc eruptions.

The Golpayegan basin is located in the Sanandaj–Sirjan zone of the Iranian plateau (Fig. 1). The seismicity of this area is directly related to active faults in the region. The scope of this research is to understand active deformation and interactions between right-lateral thrust faults and the seismicity of the study area. The Sanandaj–Sirjan zone is characterized by various tectonic segments, which have undergone long-term complex tectonic activity. The study area is a complex system of folding, thrusts, overthrusts, active reverse, right-lateral strike-slip faulting, and volcanic activity.

The quantitative method on the level of tectonic activity is determined by geomorphological indices [3–5]. The motion potential of the fault is considered a new parameter to quantify the earthquake risk for active faults. This parameter was proposed and applied by [6] for assessing the significant fault movement in the Hong Kong area. The results of this method were compatible with historical seismic records and the current microseismic activity of that region. The movement potential of active faults in the study area is determined on the basis of geometric characteristics and morphotectonic indices.

## GEOLOGICAL SETTING

The oldest rock unit in the area cropped out in the Boein and Miandasht region in an anticline with an NW–SE trend and belongs to the Upper Precambrian–Lower Cambrian age (Fig. 2) and comprises

schists, metamorphosed acid volcanic with rhyolitic composition, and crystallized limestone and dolostone intercalations in the upper part. The absence of Cambrian to Permian strata is evident in the region. Triassic–Jurassic sediments of the study area are several hundreds of dark-colored shales and siltstones deposited in a deep trough environment.

The Late Cimmerian Orogeny created a discontinuity between the Jurassic and sedimentation of the Aptian–Albian stages of the Cretaceous. The conglomerate and volcano-sedimentary rock units were deposited in the lowermost layers of the Cretaceous sequence. The Laramide orogeny, which acted as a thermodynamic phase, created tight folds and schistosity along the  $40^{\circ}$ – $60^{\circ}$  N alignment in the Cretaceous sediments. The influence of this phase has prevailed in the whole zone and has crossed over previously evolved schistosity. The Jurassic deposits are also conical in shape, with the slope of its axis towards the southeast. As we approach from northeast to southwest, the folds are more compact, and the faults are more. In the east and northwest of Golpayegan, flysch deposits can also be seen in the early Cretaceous rock units. In most of the outcrops the Jurassic and Cretaceous deposits, we can see the folding of schistosity. The folding of the schistosity surfaces is due to the subsequent phases. After the Laramide tectonic event the study area which is a part of the Sanandaj–Sirjan zone, became terrestrial and there are some Neogene clastic sediments in the southern part of the study area which are covered by Quaternary sediments.

Two groups of fault sets can be distinguished in the study area. One group is the main thrust faults with the

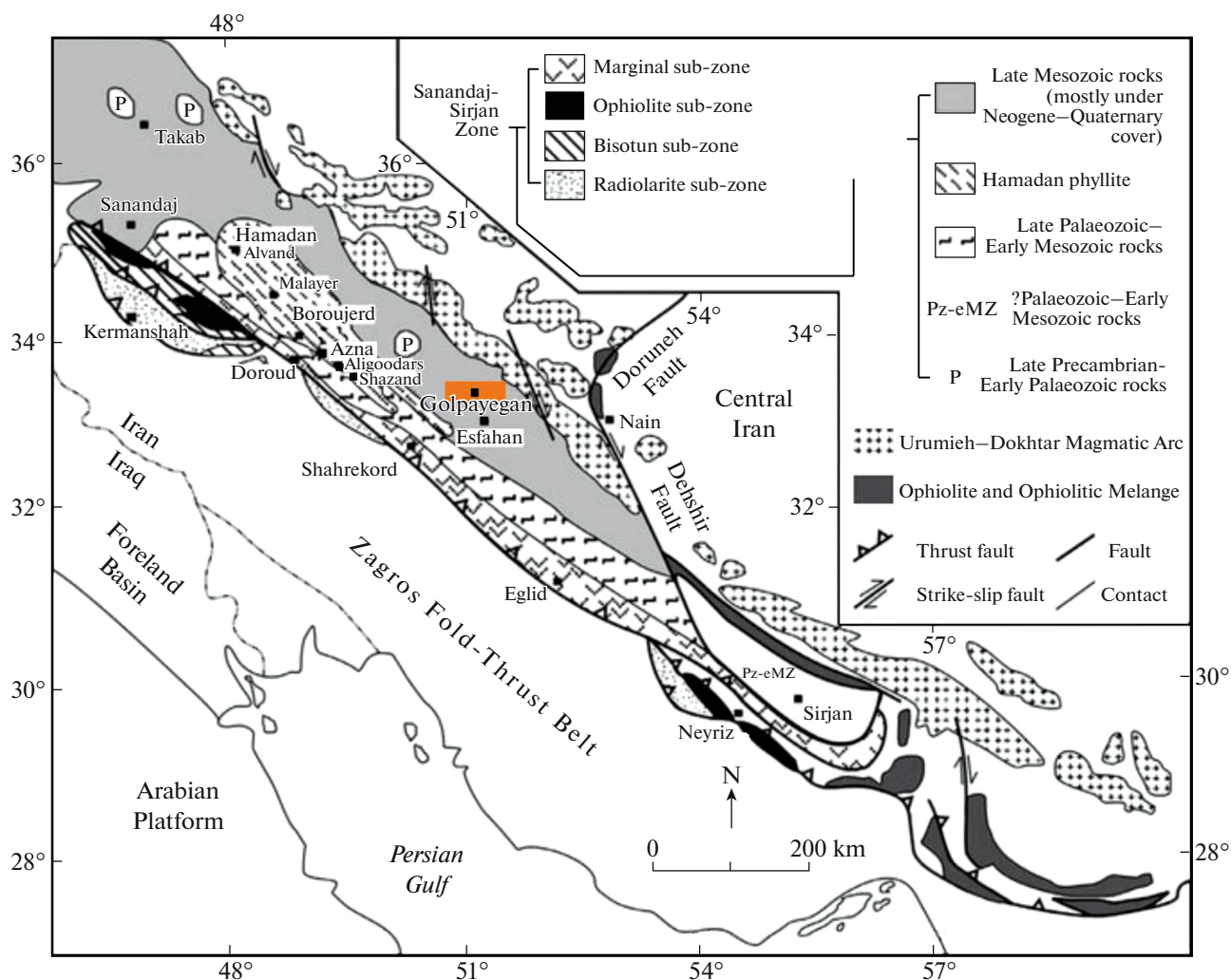


Fig. 2. Tectonic sketch map of south and western Iran, modified from [7]. The study area shown with orange color.

NW–SE trend, and the other is branches of the primary faults with the northeast-southwest direction. The Khansar, Hilla, Narpalang, Bolandab, Qarehno, and Bide Aarab faults, are six major active faults of the study area. Khansar active fault with NW–SE direction, which has approximately a length of about 60 km, passing through Jurassic and Cretaceous rock units. The Khansar and Hilla faults are parallel with a distance of less than 2 km and create a mountainous range in the central parts of the area with an NW–SE trend.

There are three parallel faults in the central part of the Sanandaj–Sirjan zone (Fig. 3). These faults are thrust-type with right-lateral components. The right lateral component of these faults can be seen in the crenulation cleavage of shear zones (Figs. 4a–4c) and the vergence of folding (Fig. 4d). Many outcrops of faults crossed-cut the quaternary sediments of the area

(Figs. 3b–3g) which in turn display the tectonic activity of the area during Quaternary.

In the area of Shazand-Golpaygan-Najaf Abad, these faults, like the Sanandaj-Sirjan area, are stretched from the southeast to the northwest and have created a tectonized range in the central part of the Sanandaj-Sirjan zone. The width of the enclosed area between these three faults is about ten kilometers. From north to south, these faults include the Bide Arab fault, Khansar fault, and Dalan fault, and they have created a high ridge with an approximate width of ten kilometers in the central part of the Sanandaj-Sirjan zone.

The Bid Arab fault is a thrust fault that is more than 200 km long and continues from the southern part of Golpaygan City to the north of Shazand City. This fault in the north of Chadegan City cuts the sediments of the alluvial fan and continues to the southeast to the city of Najaf Abad.

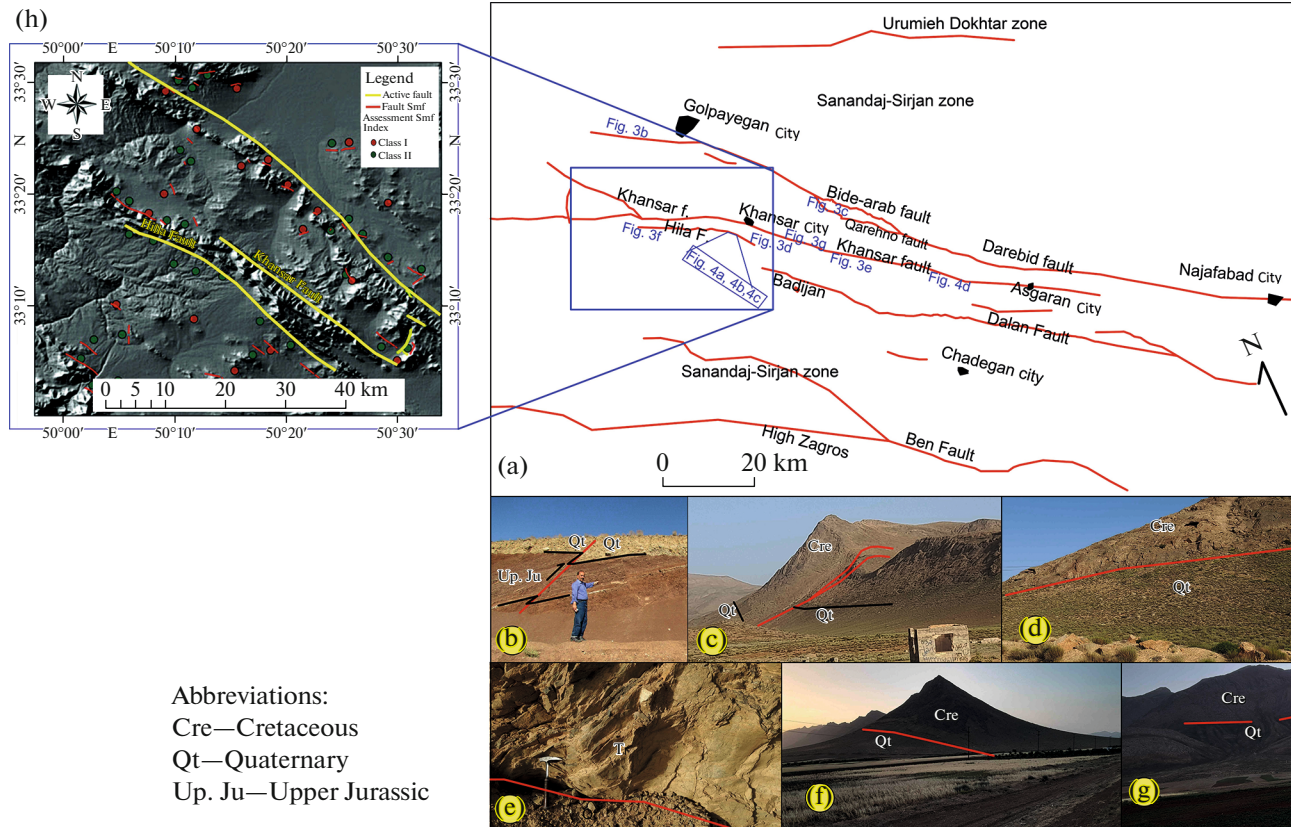


**Fig. 3.** (a) Tectonic sketch map of main thrust faults and the cities (black spots) of Sanandaj–Sirjan zone in the study area (the location of this map displayed in Fig. 2), (b) The Quaternary sediments crossed by branches of Bide Arab fault (view to east), (c) Qarehno fault (view to southwest), (d) Hila fault (view to northeast), (e) Khansar fault (view to south), (f) Hila fault (view to west), and Khansar fault (view to south), (h) Map of active faults along with mountain front faults and classification of Smf index (The Blue box of the study area).

The continuation of this fault in the Chadegan map is named as Dareh Bid fault and has caused major changes in the alluvial fans. The Qarano fault is a thrust fault that is located in the south of the Arab thrust fault and is considered a branch of the Arab fault, which is about ten kilometers long and is separated from the Arab thrust fault as a connecting supply and joins it again.

The Khansar fault system is a reverse slip diagonal fault with a right component component (Fig. 4). It starts from ten kilometers northwest of Khansar city and to the southwest continues to Asgaran, Chadegan, and Tiran towns. The Hila fault is parallel to the Khansar fault and has a distance less than 2 km away from this fault. Considering the numerous micro faults that connect these two faults, these two faults can be considered as a fault system.

The Dalan thrust fault has about 80 km in length, starts from the Badijan village, and continues from 5 km north of Chadegan city to the southeast, in the north of Chadegan city, it has had stronger effects on the Quaternary sediments, and it gradually depreciated towards the northwest.

## ACTIVE TECTONIC GEOMORPHOLOGICAL INDICES

A set of several tectonic indices can be used to investigate relative active tectonics. Using these metrics as a quantitative approach to study tectonics related to erosion and sedimentation processes in the river channel, longitudinal profile, and morphology of the river valley or tectonic features such as fault scarps and alluvial fans. Tectonic indices also can identify several zones that have been formed due to regional variations in tectonic activity.

The bifurcation indices rely on hierarchical anomalies and provide useful information about the type of erosion processes. More precisely, the hierarchical anomaly and bifurcation values of the drainage network have frequently been used as proxies for tectonic activity and are highly sensitive to the effects of tectonic activity on the geomorphic evolution.

Investigation of active tectonics e.g., [8–11] and basement faulting e.g., [12, 13] show that Iran has a high seismic potential. [14, 15] divided all rocks in Iran into several large seismotectonic units. Recent studies



by [16] in Tarom, [17] in Takab show the role of thrusts in active tectonics of Iranian territory.

Six geomorphological indices were calculated in the basins of the Golpayegan district. The results related to each index were divided [18] into three categories based on the values obtained. The average ranks of all indices related to each basin are calculated and classified into different categories, and their relative active tectonic classification map (Iat) is prepared.

#### *Drainage Basin Asymmetry Factor (Af)*

Calculating this index is a method to determine the amount of tectonic tilting in the scale of the drainage basin. This method may be used for relatively large areas [19]. An *Af* index is calculated based on the following relationship Eq. (1):

$$Af = 100 \left( \frac{Ar}{At} \right). \quad (1)$$

In this relation, *Ar* is the area on the right side of the basin (downstream view), and *At* is the area of the entire basin. If a basin is stable without tilting or with a small amount, the *Af* index equals to 50. This index is sensitive to the change in the degree of tilting in the direction perpendicular to the duct process. Values greater or less than 50 indicate basin tilting or leaning, resulting from tectonic activity or structures resulting from lithologic features. The Khoshkeh-Rud basin has the highest symmetry with a value of 51.13. The West Vaneshan and West Hezar-Jarib basins have the highest tilting due to thrusting and folding, which can be related to the active tectonic structures of the area, such as many active faults. The main trend is north-west-southeast of the region (Fig. 5a).

#### *Transverse Topographic Symmetry Factor (T)*

Calculating this index is a method to evaluate a river within the basin and the changes in the amount of asymmetry in different parts of the valley. The middle line of the basin is the place where the river is located symmetrically concerning the valley, and it is drawn according to the longest axis of the basin. For each river section, it is the ratio of the distance between the middle line to the active river (*Da*) to the distance between the middle line and the border of the basin (*Dd*) Eq. (2):

$$T = \frac{Da}{Dd}. \quad (2)$$

The evaluation of the symmetry of the drainage basins of the region using the transverse topography symmetry factor shows that, in most parts, the drainage basin is skewed. In terms of *T* value. The *T* value ranges from 0.22 for the Vaneshan basin to 0.80 for the Hilla-Ghureh basin is changing. The calculated values of the transverse topographic symmetry index align with the calculated values of the *Af* index. The *Af*

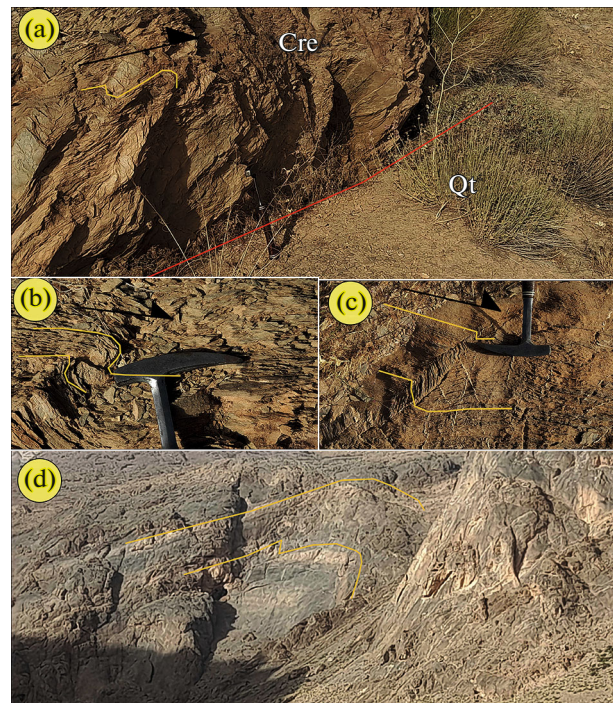


**Fig. 4.** (a) The outcrops of the Hila fault with folded cleavage in undifferentiated rocks from the late Mesozoic (view to the northeast); (b) the crumpled cleavage on the hanging wall of the Hila fault; (c) the microfolding cleavage on the hanging wall of the Khansar fault; (d) the overturned folding on the hanging wall of the Khansar fault displays the right-lateral component of the Khansar-Hila deformation zone.

index's importance confirms well the *T* index's values (Fig. 5b).

#### *Mountain-Front Sinuosity (Smf Index)*

For this research, mountain fronts were selected considering geological and geomorphological characteristics, the orientation and continuity of topography, and cross-cutting of the front by a larger drainage [20].

The Mountain-Front Sinuosity index is calculated based on the following relationship [21]:

$$Smf = \frac{Lmf}{Ls}. \quad (3)$$

In this relation Eq. (3), *Lmf* is the length of the mountain front in its range, where the slope changes between the mountain and the front basin, and *Ls* is the distance of the mountain front. Values equal to 1 of this index, are specific to tectonically active areas. In contrast, the *Smf* value increases if the uplift rate decreases and erosion processes begin to form an irregular front. Values less than 1.4 indicate active tectonic fronts [22, 23], while values greater than three are related to inactive fronts, where the fault front has eroded more than 1 km [3]. All mountain fronts in the

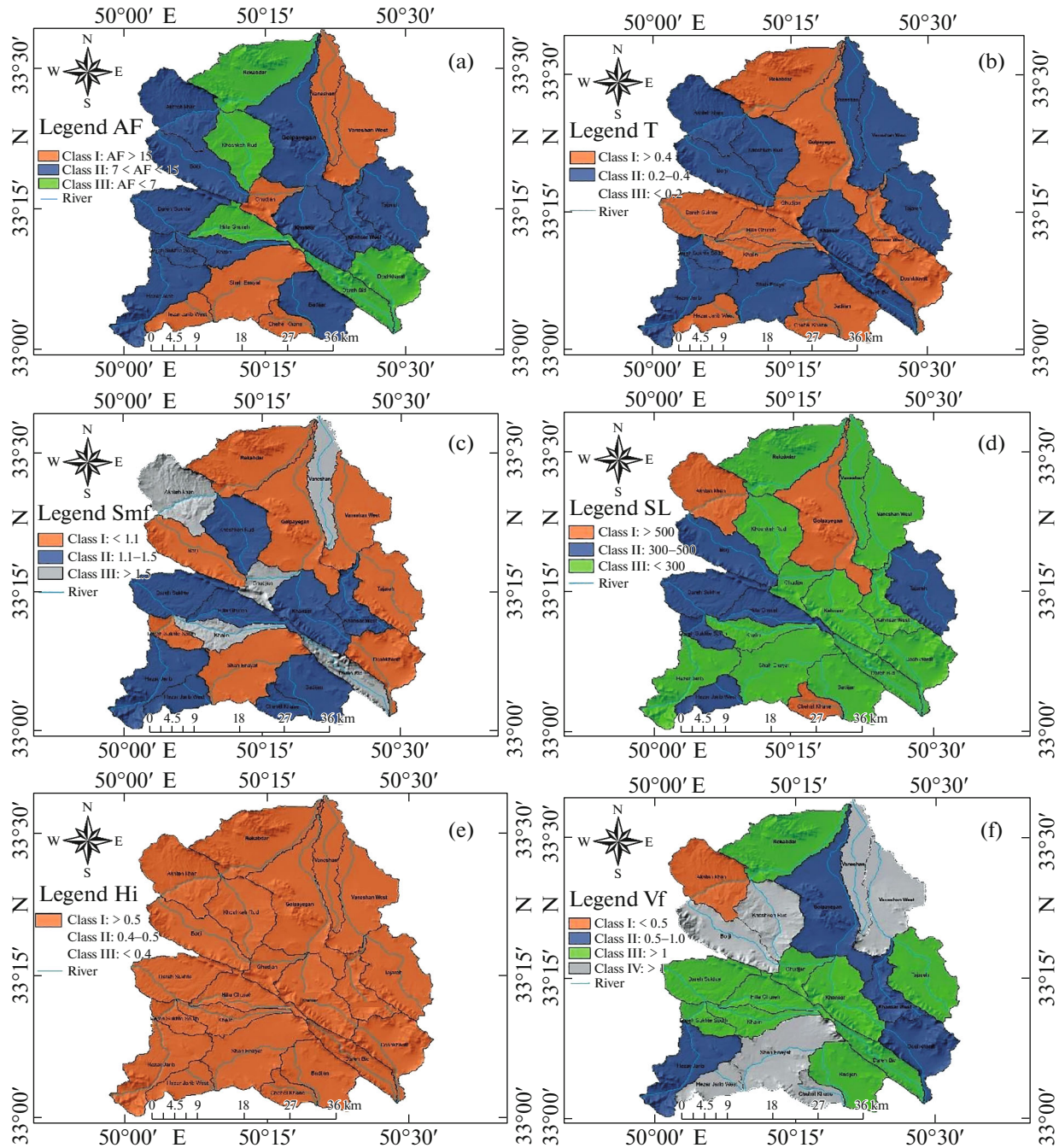


**Fig. 5.** The indices maps of the study area: (a) distribution of  $A_f$  classes; (b) distribution of  $T$  classes; (c) distribution of  $Smf$  classes; (d) distribution of  $SL$  classes; (e) distribution of  $H_i$  index; (f) distribution of  $V_f$  classes.

region are classified as very active fronts, and all points are in tectonic category one because  $Smf$  values are less than 1.5. The obtained data show that the two basins of Golpayegan and Dareh-Sukhte-South Valley have the most active parts in the whole region and are characterized by very active mountain fronts that can be related to active tectonic structures in these areas (Fig. 5c).

#### Stream Length-Gradient Index ( $SL$ Index)

The river length-slope index was described by [24] as follows Eq. (4):

$$SL = \frac{\Delta H}{\Delta L} L, \quad (4)$$

where  $\Delta h$  is change in altitude,  $\Delta L$  is length of a reach, and  $L$  is the horizontal length from the watershed

divide to midpoint of the reach. In this relation,  $\frac{\Delta H}{\Delta L}$  is the slope of a part of the conduit, and  $L$  is the length of the conduit from upstream to the point for which the index is calculated. This index is useful for evaluating relative active tectonics.

When rivers and streams flow in areas with high upwelling rates, the value of  $SL$  increases. Meanwhile, when the river flows parallel to structures such as valleys resulting from strike-slip faults, the amount of  $SL$  decreases [5]. The values of this index in the study area were calculated using a digital elevation model and geographic information system; the three basins of Golpayegan, Chehel-khaneh, and Akhteh-Khan have relatively high Stream Length Gradient Index (Fig. 5d).

#### Hypsometric Integration ( $H_i$ )

Hypsometric Integration is an index that shows height dispersion in a specific area. Normally, the integral is calculated for a specific drainage basin and is independent of the area of that basin. A simple relationship is used to calculate this index [25, 26] as follows Eq. (5):

$$H_i = \frac{\text{average elevation} - \text{min.elevation}}{\text{max.elevation} - \text{min.elevation}}. \quad (5)$$

The necessary data for calculating Hypsometric Integration is prepared from the elevation-digital model of the area; the average elevation is obtained by randomly selecting 50 elevation points in the basin, and the value of this index is equal to the area under the surface of the hypsometric curve. Hypsometric integration is not directly related to the active ground. Active and newly formed tectonic regions are associated with high values of this index. In contrast, its low values are related to old sites that have suffered a lot of erosion and are less affected by dynamic and young tectonics [18]. In the study area, the elevation curves for the basins were drawn by Excel software, and the hypsometric integration values for the study area's basins were calculated by estimating the area beneath the elevation curves' surface.

High  $H_i$  index values indicate the active tectonic state or the early stage of the Davis pattern, which has been observed in all the basins of the study area. All the region's basins are in category 1 of relative tectonic activity (Fig. 5e).

#### The Ratio of Valley Floor width to Valley Height ( $V_f$ )

Index  $V_f$  as the ratio of valley floor width to its height, is described as follows Eq. (6):

$$V_f = \frac{2V_{fw}}{(E_{LD} - E_{SC}) + (E_{rD} - E_{SC})}. \quad (6)$$

In this relationship,  $V_{fw}$  is the width of the valley floor,  $E_{LD}$  is the height of the left wall of the valley,  $E_{rD}$  is the height of the right wall of the valley, and  $E_{SC}$  is the average height of the valley floor. The value of this index is high for U-shaped valleys and low for narrow and steep V-shaped valleys. Considering that the elevation is related to the amount of excavation of the valley, the low value of  $V_f$  corresponds to the areas with a high uplift rate. According to [5],  $V_f$  is calculated at a certain distance from the fault front. In the Doshkharat basin, point one with the lowest  $V_f$  value is the most active point in all the study basins and is represented by a V-shaped valley, and in the Khansar basin at point six, the  $V_f$  value is the highest in all study basins and is characterized by a U-shaped valley. The shape is determined according to the calculations of the  $V_f$  index. The Akhteh Khan basin is in the first category of relative tectonic activity (Fig. 5f).

#### Drainage Basin Shape

The horizontal projection of a basin is described by the Drainage basin shape index or the elongation ratio [27, 28], The  $B_s$  can be determined by [18] as follows Eq. (7):

$$B_s = \frac{Bl}{Bw}, \quad (7)$$

where  $Bl$  is the length of the basin measured from its mouth to the most distant drainage divide and  $Bw$  denotes the width of a basin measured at its widest point. The Drainage basin shape ( $B_s$ ) index map of the study area is presented in (Fig. 6).

#### Classification of Relative Tectonic Activity ( $Iat$ )

This paper is the classification of relative active tectonics that [18] published for the first time. In this research, the evaluation of the relative active tectonics ( $Iat$ ) of the basins of the studied area was carried out.

Different geomorphological indices calculated for each basin are divided into three categories, Category 1 indicates very high activity, Category 2 indicates high activity, and Category 3 shows moderate activity. Relative active tectonic values ( $Iat$ ) were calculated for the basins of the studied area by averaging them and rounding the numbers (Fig. 7).

#### THEORETICAL MODEL FOR FAULT MOVEMENT POTENTIAL ANALYSIS

Fault movement potential (FMP) is dependent on tectonic stress ( $\sigma$ ), fault plate geometry ( $G$ ), and physical properties of the inner and side of the fault ( $P$ ). FMP is a function of these factors [6]:

$$FMP = f(\sigma, G, P). \quad (8)$$



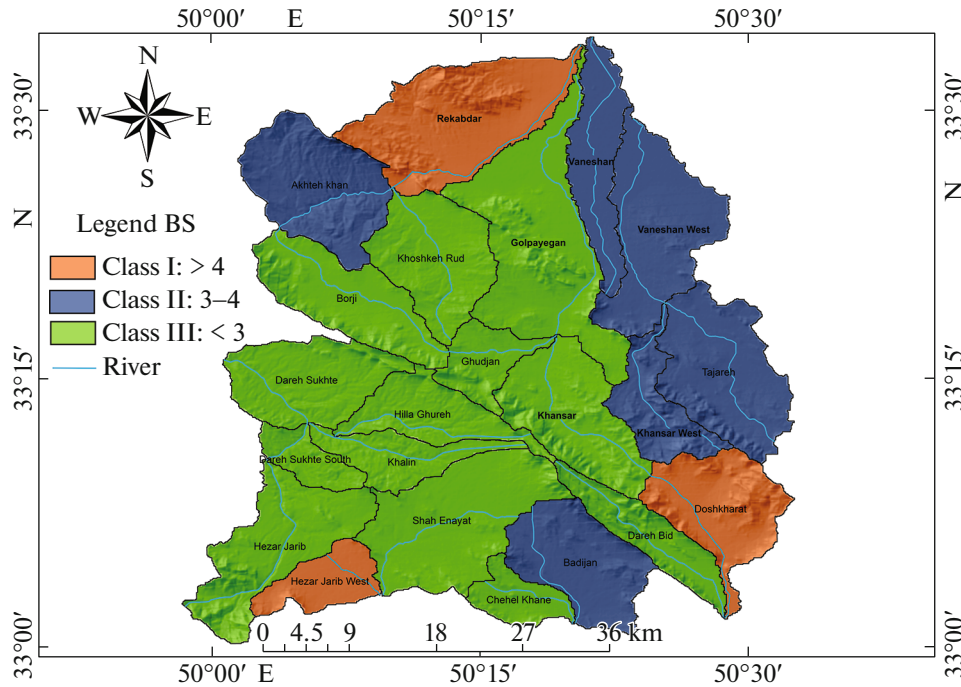


Fig. 6. The Drainage basin shape (*Bs*) index map of the study area.

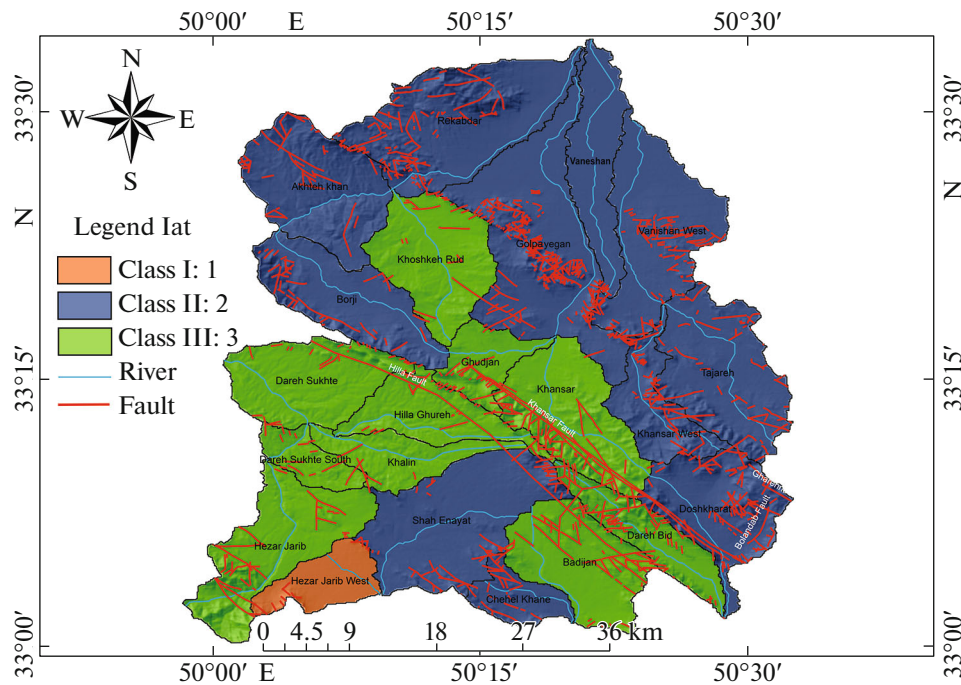


Fig. 7. The Iat index map of the study area.

Although a geological environment is usually heterogeneous and complicated, it can be considered statistically homogeneous and isotropic. Based on this problem and to simplify the theoretical model, the geological environment of the faults is regarded as a

homogeneous, isotropic, and elastic material. Thus, FMP can be simplified as follows

$$FMP = f(\sigma, G). \tag{9}$$



To consider the effect of tectonic stress orientation and fault geometry on fault seismicity, [6] conducted experiments using block models. The results show that changing the slope of the fault causes significant changes in the time intervals of the reoccurrence of seismic events, independent of the amount of seismic energy. For some slope values, the seismic activity of the fault disappears, and to prove the results of these experiments, [6] conducted a theoretical analysis and showed that the faults could slip when the angles are between 20 and 70 degrees in the orientation of the maximum compressive stress and along the fault. However, there are some exceptions to this model for real fault systems. These exceptions are due to the limitation of two-dimensional investigations. Fault planes are not always vertical, and the orientation of the maximum compressive stress is not always horizontal. This problem is considered using Moore's stress circle in this method.

### THE ORIENTATION OF REGIONAL TECTONIC STRESS

Tectonic stress is a stress added to the lithostatic stress condition. In other words, the deviated part is dedicated to the lithostatic stress. Analyzing the depth mechanism of earthquakes is one of the most common methods in studying contemporary tectonic stress. However, the main compressive stress orientation maximally obtained from the analysis of the deep mechanism of a strong earthquake represents the characterization of a large regional tectonic stress field. Some analyses of the deep mechanism of large earthquakes reveal the complex conditions of deep structures and the view of stress. The stress view means that the exceptional stress field in the instantaneous focal process is added to the regional tectonic stress field in earthquake creation. The analysis of the depth mechanism of a single small earthquake has a random shape. Fortunately, analyses of the artificial depth mechanism of many small earthquakes may determine the condition of regional tectonic stress. Thus, both the analysis of the depth mechanism of large earthquakes and the average analysis of small earthquakes can be used to obtain the overall composition of the regional stress situation. The assessment of the movement potential of Quaternary faults shows that even without a known history of seismicity, it is possible to rank active faults based on the parameter mentioned above. Since we do not have the solution of the focal mechanism of earthquakes in this area, based on the dynamic investigation of fractures and joints and their averaging, the direction of the maximum main stress was obtained.

To achieve the dynamic analysis of active faults in the Golpayegan region, the shear surfaces with sliding Lineaments and their related fault planes were measured, and the results were compared with some other geological phenomena such as injection planes, Stylo-

**Table 1.** Calculations of kinetic power of active faults in Golpayegan region using regional stress

Fault name	Fault plane	( $\sigma_1$ )	$\theta$	FMP
Narpalang Fault	312/71	270/50	46	0.5
Bolandab Fault	243/62	270/50	80	0.3
Qarehno Fault	325/64	270/50	35	0.1
Bide Aarab Fault	110/60	270/50	55	0.8
Khansar Fault	319/73	270/50	45	0.5
Hilla Fault	321/69	270/50	42	0.4

lites, and cumulative process. The minerals were controlled, and finally, the changes in the direction of stress in the rock units were calculated; for this purpose, the inversion method was used to determine the direction of the principal stress axes, and at all points, the main stresses of the region were calculated by Tectonics FP software. This method assumes that the scratches on the fault plane indicate the direction of the maximum shear pressure. Finally, the angle of the plane's average vector to the maximum main stress was measured by meaning ( $\sigma_1 = 270/50$ ) and inserted into the equations of Table 1. The movement potential of active faults in the area was obtained at each section. In the approach used by [6], the movement potential of active faults in the study area, with regional stress in each section, was calculated separately. All regional stress calculations were solved using Eq. (10) (Table 1). After performing the calculations, the results obtained from the method of [6], that is, the solution of the equation based on regional stress, were compared with those obtained from seismic data.

$$FMP = \begin{cases} 0 & \theta \in (0^\circ, 30^\circ) \\ \frac{\theta - 60^\circ}{30^\circ} & \theta \in (30^\circ, 60^\circ) \\ 1 - \frac{\theta - 60^\circ}{30^\circ} & \theta \in (60^\circ, 90^\circ), \end{cases} \quad (10)$$

$\theta$  is the angle between the regional maximum principal compressive stress orientation ( $\sigma_1$ ) and the normal line of fault plane and FMP is fault movement potential.

### CONCLUSIONS

According to the calculations of the geomorphic parameters in the study area, the four basins of Golpayegan, Doshkharat, Darehbid, and East Hezar-Jarib basin determined as the most active basins in the entire study area and are characterized by very active mountain fronts. According to El-Hamdouni's (2008)

model, except for these four basins, with very high relative tectonic activity, other parts of the study area consist of zones with high to medium activity with 2nd (moderate) to 3rd activity categories. The Ghudjan, Shah Enayat, Chehel-khane, west Vaneshan, and Vaneshan basins have moderate tectonic categories. The morphometric data provided evidence for relative variations in tectonic activity among the Golpayegan basin. a relatively high degree of tectonic activity along the western part of the Golpayegan city, in a zone parallel to the main thrust of Zagros. The computation of morphometric indices in Golpayegan basin means that tectonic activity is remarkable from Morphometric point of view. Tectonic activity is not been the same throughout the region, although no major earthquakes have been reported in the Golpayegan area, but the morphometric evidence indicates the overall activity of tectonic setting of the region; so, it's good to keep in mind it, considering presence of faults in this area, and the age of the seismic recorders respect to geomorphic features. Geomorphic evaluation of the Golpayegan region suggests that some NW-SE trending faults, and specifically the tips of some faults at the west the Golpayegan city, should be considered as areas of potentially earthquake risk.

The southern part of the Bide Aarab Fault is associated with the highest movement activity potential and the youngest neotectonics' evidence. The frequency of earthquakes around the Hilla and Khansar faults, which are parallel with a distance of less than 2 km, displays a high-activity seismic zone with an NW-SE trend in the central part of the area. The values of bifurcation indices revealed that the calculated movement potential of the faults corresponds well to the areas with frequency of earthquakes and landforms such as deflected and offset streams, and deformed Quaternary sediments that indicate the post-Neogene activity, and demonstrated that these landforms were created by movements along the main faults such as Bid Arab and Khansar faults which have the highest mobility potential in the future.

#### ACKNOWLEDGMENTS

We acknowledge department of earth sciences, Islamic Azad university, Tehran for their cooperation during the study.

#### AUTHOR CONTRIBUTION

All authors contributed to the study conception and design, material preparation, data collection and analysis. All of them read and approved the final version of manuscript.

#### FUNDING

This work was supported by ongoing institutional funding. No additional grants to carry out or direct this particular research were obtained.

#### CONFLICT OF INTEREST

The authors of this work declare that they have no conflicts of interest.

#### REFERENCES

1. J. Eftekharnjad, J. Iran. Petrol. Soc. **82**, 19–28 (1981).
2. J. Rahnamarad, G. Farhoudi, H. Ghorbani, S. Habibi-mood, and R. Derakhshani, Iran. J. Earth Sci. **1** (1), 57–72 (2009).
3. W. B. Bull and L. D. McFadden, in *Proc. 8th Annu. Geomorphol. Symp. Geomorphology in Arid Regions*, Ed. by D. O. Doehring (State University of New York, Binghamton, 1977), pp. 115–138.
4. A. Azor, E. A. Keller, and R. S. Yeats, Geol. Soc. Am. Bull. **114** (6), 745–753 (2002).
5. E. Keller and N. Pinter, *Active Tectonics, Earthquakes, Uplift and Landscape* (Prentice Hall, Englewood Cliffs, 2001).
6. C. F. Lee, J. J. Hou, and H. Ye, Episodes **20** (4), 227–231 (1997).
7. M. Mohajjel, C. L. Fergusson, and M. R. Sahandi, J. Asian Earth Sci. **21**, 397–412 (2003).
8. M. Arian, Carbonates Evaporites **27**, 9–18 (2012).
9. M. Arian and Z. Aram, Solid Earth, No. 2, 1277–1291 (2014).
10. J. Ehsani and M. Arian, Geoscience J. **19**, 1–15 (2015).
11. Z. Aram and M. Arian, Episodes **39**, 39–44 (2016).
12. M. Arian, H. Alizadeh, and H. Noroozpour, Indian J. Sci. Tech. **4** (10), 1303–1306 (2011).
13. M. Arian, N. Bagha, R. Khavari, and H. Noroozpour, Indian J. Sci. Technol. **5**, 2379–2383 (2012).
14. M. Arian, Earth Sci. Res. J. **19**, 7–13 (2015).
15. G. Razaghian, A. Beitollahi, M. Pourkermani, and M. Arian, J. Geodyn. **119**, 29–46 (2018).
16. R. Nouri, M. R. Jafari, M. Arian, F. Feizi, and P. Afzal, Arch. Min. Sci. **58**, 1071–1084 (2013).
17. R. Nouri and M. Arian, Arab. J. Geosci. **10** (5), 105–110 (2017).
18. R. El-Hamdouni, C. Irigaray, T. Fernandez, J. Chacón, and E. A. Keller, Geomorphology **96** (1-2), 150–173 (2008).
19. P. W. Hare and T. W. Gardner, in *Proc. 15th Annu. Binghamton Geomorphol. Symp. Tectonic Geomorphology*, Ed. by M. Morisawa and J. T. Hack (Allen and Unwin, Boston, 1985), pp. 123–134.
20. S. G. Wells, T. F. Bullard, T. M. Menges, P. G. Drake, P. A. Karas, K. I. Kelson, J. B. Ritter, and J. R. Wesling, Geomorphology **1**, 239–265 (1988).
21. W. B. Bull, *Tectonic Geomorphology of Mountains: A New Approach to Paleogeomorphology California* (Blackwell, Malden, 2007).

22. T. K. Rockwell, E. A. Keller, and D. L. Johnson, in *Proc. 15th Annu. Geomorphol. Symp. Tectonic Geomorphology*, Ed. by M. Morisawa (Allen and Unwin Publ., Boston, 1985), pp. 183–207.
23. E. A. Keller, in *Active Tectonics, Studies in Geophysics*, Ed. by R. E. Wallace (Natl. Acad. Press, Washington, 1986), pp. 136–147.
24. J. T. Hack, *J. Res. U.S. Geol. Surv.* **1**, 421–429 (1973).
25. R. J. Pike and S. E. Wilson, *Geol. Soc. Am. Bull.* **82**, 1079–1084 (1971).
26. L. Mayer, *Introduction to Quantitative Geomorphology* (Prentice Hall, Englewood, Cliffs, 1990).
27. P. J. Cannon, *Oklahoma Geol. Notes* **36** (1), 3–16 (1976).
28. M. T. Ramírez-Herrera, *Earth Surf. Process. Landforms* **23**, 317–332 (1998).

**Publisher's Note.** Pleiades Publishing remains neutral with regard to jurisdictional claims in published maps and institutional affiliations.